

## Further studies of a simple atomistic model of silica: Thermodynamic stability of zeolite frameworks as silica polymorphs

Matthew H. Ford

*Department of Chemical Engineering, University of Massachusetts, Amherst, Massachusetts 01003*

Scott M. Auerbach

*Department of Chemical Engineering and Department of Chemistry, University of Massachusetts, Amherst, Massachusetts 01003*

P. A. Monson<sup>a)</sup>

*Department of Chemical Engineering, University of Massachusetts, Amherst, Massachusetts 01003*

(Received 1 November 2006; accepted 6 February 2007; published online 9 April 2007)

We have applied our previously reported model of silica based on low coordination and strong association [J. Chem. Phys. **121**, 8415 (2004)], to the calculation of phase stability of zeolite frameworks SOD, LTA, MFI, and FAU as silica polymorphs. We applied the method of Frenkel and Ladd for calculating free energies of these solids. Our model predicts that the MFI framework structure has a regime of thermodynamic stability at low pressures and above  $\sim 1400$  K, relative to dense phases such as quartz. In contrast, our calculations predict that the less dense frameworks SOD, LTA, and FAU exhibit no regime of thermodynamic stability. We have also used our model to investigate whether templating extends the MFI regime of thermodynamic stability to lower temperatures, by considering templates with hard-sphere repulsions and mean-field attractions to silica. Within the assumptions of our model, we find that quartz remains the thermodynamically stable polymorph at zeolite synthesis temperatures ( $\sim 400$  K) unless unphysically large template-silica attractions are assumed. These predictions suggest that some zeolites such as MFI may have regimes of thermodynamic stability even without template stabilization. © 2007 American Institute of Physics. [DOI: [10.1063/1.2712440](https://doi.org/10.1063/1.2712440)]

### I. INTRODUCTION

Zeolites are nanoporous crystalline aluminosilicates with a rich variety of interesting properties and industrial applications.<sup>1</sup> The ordering of channels and cavities in zeolites has been exploited for many years to produce selective reactions and separations. Despite the wide application of zeolites, understanding how zeolites crystallize and what makes them stable remains an elusive but important goal of zeolite science. A prevailing view in the literature on zeolites is that all-silica zeolite frameworks do not represent thermodynamically stable polymorphs of silica, but rather are local minima of the free energy.<sup>2</sup> Of course, once in such a local minimum, the system will remain there indefinitely if the free energy barriers to be crossed are sufficiently high. In this picture, the use of a template or structure-directing agent (SDA) in zeolite synthesis is a means of trapping the silica into an open-framework structure with channels and cavities. It is worthwhile to ask whether this view is generally correct, considering that thermochemistry measurements of zeolite formation find that zeolite instability decreases with temperature,<sup>3,4</sup> suggesting that under certain circumstances zeolites might be thermodynamically stable relative to dense phases such as quartz. We address this question by applying molecular simulations of a model of silica to examine

whether all-silica zeolite frameworks SOD, LTA, MFI, and FAU exhibit regimes of thermodynamic stability in the silica phase diagram.

The thermodynamic stability of pure silica zeolites has been studied by experimental calorimetry<sup>3-7</sup> and molecular modeling.<sup>8-15</sup> Most modeling studies report potential energy optimizations, while most experiments measure lattice enthalpies. The main conclusions from these studies are that (i) silica zeolite energies are found in the range  $10 \pm 4$  kJ per mol  $\text{SiO}_2$  above that of quartz, and (ii) the energy variation among silica zeolites correlates with framework density. These findings are consistent with the results of classical theory,<sup>14</sup> classical simulations,<sup>9,12</sup> and quantum density functional theory calculations.<sup>8</sup> This range of energies is rather narrow considering the breadth of Si-O-Si angles exhibited by zeolite frameworks, from  $140^\circ$  to  $180^\circ$ .<sup>16</sup> Such a narrow range of energies inspired our base-case model of silica<sup>17</sup> (see below), which assumes that all completely bonded (i.e.,  $Q_4$ ) silica polymorphs are isoenergetic, regardless of structure. This picture is supported by our periodic density functional theory (DFT) calculations on five dense and five zeolitic silica polymorphs;<sup>8</sup> the electronic energies of these ten polymorphs were found to be within 7.7 kJ per mol  $\text{SiO}_2$  of quartz. Below we discuss results from the isoenergetic model,<sup>17</sup> and investigate corrections to this model accounting for finer details of silica energetics based on our DFT calculations.<sup>8</sup>

Relatively few studies have reported Gibbs free energies

<sup>a)</sup>Electronic mail: monson@ecs.umass.edu

of silica zeolite frameworks. Such free energies are necessary for constructing thermodynamic phase diagrams, which can shed light on phase stability assuming that zeolite formation is thermodynamically controlled. Piccione *et al.* measured Gibbs free energies of zeolite crystallization with occluded SDAs for various zeolite/SDA combinations.<sup>7</sup> For MFI/TPA (tetrapropyl-ammonium), Piccione *et al.* report a zeolite-SDA crystallization free energy from solution of  $-8.1 \pm 2.8$  kJ per mol  $\text{SiO}_2$ , suggesting that this process may be driven to some extent by thermodynamics (the question remains why the synthesis does not produce quartz). Focusing on silica frameworks, Johnson *et al.* measured Gibbs free energies of various silica phases at 298 and 1000 K,<sup>3</sup> the results for silica MFI (relative to quartz) are 4.1 and 1.4 kJ per mol  $\text{SiO}_2$ , respectively. These data suggest that MFI approaches thermodynamic stability at elevated temperatures, and might even become stable at temperatures higher than 1000 K. Vieillard used simple ion packing arguments to estimate the Gibbs free energy of silica MFI relative to quartz, finding 8.5 kJ per mol  $\text{SiO}_2$  at 298 K.<sup>14</sup> Wu and Deem<sup>15</sup> applied molecular simulations to compute the Gibbs free energy difference between silica MFI and quartz using a modified version of Vashishta's forcefield.<sup>18</sup> Wu and Deem report a free energy difference of 58.6 kJ per mol  $\text{SiO}_2$  at 298 K, a result well above the expected range for silica polymorphs. This suggests that more work is needed to develop an atomic-level understanding of the thermodynamic stabilities of dense and zeolitic silica polymorphs.

We have developed a simple atomistic model of silica that gives a qualitatively accurate picture of silica phase behavior, while remaining computationally efficient.<sup>17</sup> Such efficiency is important, given that free energy calculations for model potentials of silica<sup>18–22</sup> can be quite computationally intensive, which makes it challenging to obtain statistical convergence. In our model, we view silica as a material dominated by low coordination and strong association, inspired by previous models of hydrogen bonded fluids.<sup>23,24</sup> For computational efficiency, these interactions were implemented through hard-sphere repulsions and directional square-well attractions. In Ref. 17, we also reported free energy calculations using the method of Frenkel and Ladd<sup>25</sup> applied to our model, giving good qualitative agreement with experimental phase data for the dense silica phases, as well as for their mechanical properties. In the present article, we investigate the thermodynamic stability of several all-silica zeolite frameworks as polymorphs of silica, within the context of this model.

SDAs play a critical role in controlling zeolite formation, and in allowing relatively mild synthesis conditions.<sup>2,26,27</sup> Zeolite scientists have considered the possibility that SDAs may even provide thermodynamic stability to zeolite frameworks.<sup>15</sup> That is, although quartz is the thermodynamically stable polymorph of silica in air at room temperature, the zeolite-SDA complex may be thermodynamically stable relative to quartz/SDA in solution under synthesis conditions. To investigate the thermodynamic stabilization of silica zeolites by SDAs, a suitable model of the silica-SDA interaction is required. Previous simulations of SDAs have used detailed, atomistic models showing how

SDAs interact with zeolite pores<sup>28,29</sup> or silicate solutions.<sup>30</sup> Most of these simulations involve potential energy optimizations for SDAs in known zeolite pores.<sup>28,29</sup> Such detailed models are important for shedding light on the delicate relationship between SDA structure and zeolite framework topology. Instead, we study a more generic issue, for which we build a generic model. We examine whether silica-SDA interactions can make a zeolite-SDA complex thermodynamically stable (relative to quartz) at zeolite synthesis temperatures. As a base case for this study, we investigate hard-sphere templates that experience mean-field attractions to silica. This choice of model offers the following benefits: (i) It is consistent with the spirit of our model for silica, (ii) it allows the separate study of silica-SDA attractions and repulsions, and (iii) it allows statistically converged free-energy calculations. In future work, we plan to study SDAs with more complex structures, and with more site-specific silica-SDA attractions.

Below we report the surprising prediction that all-silica MFI has a regime of thermodynamic stability within our model, relative to dense phases such as quartz. Our model also predicts that quartz remains the thermodynamically stable polymorph at zeolite synthesis temperatures ( $\sim 400$  K) unless unphysically large MFI-SDA attractions are assumed. The remainder of this article is organized as follows: In Sec. II we describe the model and the free energy calculations used to construct phase diagrams; in Secs. III A and III B, we discuss results of phase diagrams for dense and zeolitic silica polymorphs without SDAs; in Secs. III C and III D, we discuss our findings for templated frameworks; and in Sec. IV we offer concluding remarks.

## II. MOLECULAR MODEL AND CALCULATION METHODS

### A. Silica model

Our model represents silicon as a hard sphere with four square well association sites tetrahedrally arranged on its surface.<sup>17</sup> This enforces the tetrahedral coordination of oxygen atoms about a single silicon atom. Oxygen is modeled as a hard sphere with two square well sites on its surface. The angle between the bonding sites on oxygen is fixed at  $145.8^\circ$ . This value is the average of the Si–O–Si angles exhibited in  $\alpha$ - and  $\beta$ -phases of quartz and cristobalite. Si–O–Si angles larger and smaller than this are possible because of the finite range of the bonding interactions used in the model.

The silicon-silicon and silicon-oxygen repulsions are modeled with hard-sphere potentials defined by the hard-sphere diameter  $\sigma$ . The oxygen-oxygen interaction is modeled with a hard-sphere diameter of  $1.6\sigma$ . This diameter non-additivity helps reproduce the O–Si–O bond angle distribution predicted by molecular-dynamics simulations.<sup>18</sup> The silicon-oxygen bonded interaction is modeled as a square well potential, i.e.,

$$u_{\text{sw}}(r_{\text{site-site}}) = \begin{cases} -\epsilon & r_{\text{site-site}} \leq \lambda \\ 0 & r_{\text{site-site}} > \lambda \end{cases} \quad (2.1)$$

We use the largest value of  $\lambda$  that allows only one bond to form between any two bonding sites. This value is given by

$\lambda = (1 - \sqrt{3}/2)\sigma$ ,<sup>24</sup> and permits Si–O–Si angles from about 130° up to 180° in a fully bonded structure. The average Si–O bond length in our model is thus  $\sigma + (\lambda/2) = \sigma(1.5 - \sqrt{3}/4)$ . Equating this to the standard Si–O bond length of 1.6 Å gives  $\sigma = 1.5$  Å. The well depth  $\varepsilon$  represents the Si–O bond dissociation energy, which is  $\sim 380$  kJ per mol.<sup>31</sup>

For all fully bonded silica polymorphs, our model assumes an energy of  $E = -4N_i\varepsilon$ , where  $N_i$  is the number of SiO<sub>2</sub> formula units in the simulation cell of the  $i$ th polymorph (e.g., 192 for FAU). The normalized energy,  $E/N_i = -4\varepsilon$ , is thus the same for all polymorphs within our present model. As discussed above, this is qualitatively consistent with experimental and computational data.<sup>3–15</sup> However, we can investigate the impact of subtle differences in the energy among polymorphs by adding ground-state corrections from our DFT calculations<sup>8</sup> via the ansatz

$$E_i/N_i = E_0(i) - 4\varepsilon, \quad (2.2)$$

where  $E_0(i)$  is the normalized ground-state electronic energy of the  $i$ th polymorph. The dense phases we consider are quartz, cristobalite and coesite; the zeolitic phases treated are SOD, LTA, MFI, and FAU.<sup>16</sup> Several DFT-calculated ground-state energies of silica polymorphs can be found in Table X of Ref. 8; the corrections used in the present study are:  $E_0(\text{quartz}) = 0$ ,  $E_0(\text{cristobalite}) = 2.9$  kJ per mol SiO<sub>2</sub>, and  $E_0(\text{MFI}) = 4.8$  kJ per mol SiO<sub>2</sub>. [No correction for coesite was computed in Ref. 8; as such, we take  $E_0(\text{coesite})$  to be zero.] Below we compare silica phase diagrams with and without these corrections, to determine how they impact phase stability.

## B. Template model

As discussed in the Introduction, we also study the influence of silica-SDA interactions on the phase stability of the MFI-SDA complex. Our model involves hard-sphere SDAs that experience mean-field attractions to silica. We pursue this generic model to investigate fundamental questions about SDA stabilization of silica polymorphs. To shed light on the separate influences of silica-SDA attractions and repulsions, we first consider only hard-sphere templating; we then consider both hard-sphere repulsions and mean-field attractions. The hard-sphere interaction is given by

$$u_{\text{TF}}(r) = \begin{cases} \infty & r \leq \sigma_{\text{TF}} \\ 0 & r > \sigma_{\text{TF}} \end{cases}. \quad (2.3)$$

We have chosen  $\sigma_{\text{TF}} = 4\sigma_{\text{Si-O}}$ , which we found localizes SDAs to MFI channel intersections. In computing the phase diagram for systems with the SDA, we make use of the well-known equations of state of hard-sphere solids and fluids.<sup>32</sup>

We augment these repulsions by mean-field SDA-framework attractions. Assuming no hard-sphere SDA-framework contacts, the overall SDA-framework interaction is  $-M_i\varepsilon_{\text{TF}}$ , where  $M_i$  is the number of SDA molecules in the simulation cell of the  $i$ th polymorph (e.g., four for MFI), and  $\varepsilon_{\text{TF}}$  is the strength of attraction between the framework and each SDA molecule. To determine initial locations for the four SDAs in MFI, the empty MFI framework was probed

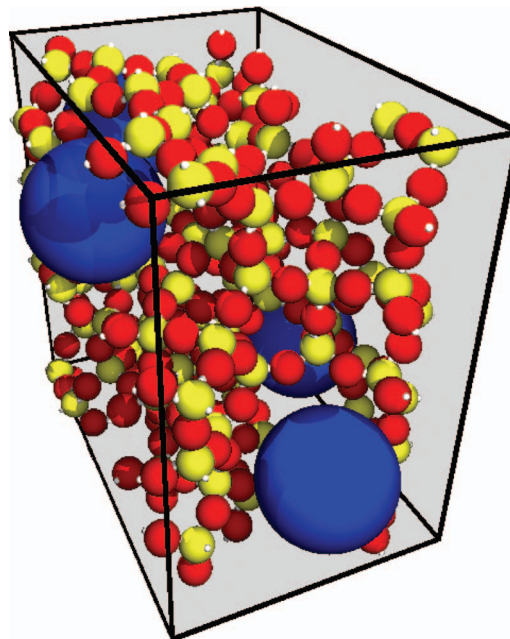


FIG. 1. (Color) Single unit cell of MFI with four template molecules each located at a channel intersection.

with a hard sphere by scanning over a grid to search for locations that avoid hard-sphere overlap. The size of the probe hard sphere was increased and the mesh refined until only four overlap-free locations were found. Figure 1 shows a unit cell of MFI with four SDA molecules. The SDA locations are listed as fractional coordinates in Table I.

## C. Free energy and phase equilibrium calculations

We refer the reader to our previous paper<sup>17</sup> for a description of the pure silica free energy calculations. In brief, these were performed using thermodynamic integration from a harmonic (Einstein) solid reference system, according to the Frenkel-Ladd methodology.<sup>25</sup> Sampling the orientations of silicon and oxygen atoms requires special care, because of the anisotropy associated with the bonding sites on these atoms.

To investigate the effect of SDAs on the silica phase diagram, we introduce the templated silica and pure template (hard-sphere) phases into the free energy calculations. We treat templated MFI as a substitutionally ordered solid compound for which the Frenkel-Ladd methodology<sup>25</sup> remains valid.<sup>33</sup> For the dense silica phases, inside which the SDA cannot fit, we assume there is no mixing between the SDA and silica. As such, we construct phase diagrams with the following regions: (1) Separate MFI and template, (2) separate cristobalite and template, (3) separate quartz and template, and finally, (4) templated MFI, i.e., the compound

TABLE I. Fractional coordinates of the template molecules.

Molecule	1	2	3	4
$x$	0.016	0.476	0.516	0.976
$y$	0.752	0.252	0.752	0.252
$z$	0.368	0.868	0.076	0.576

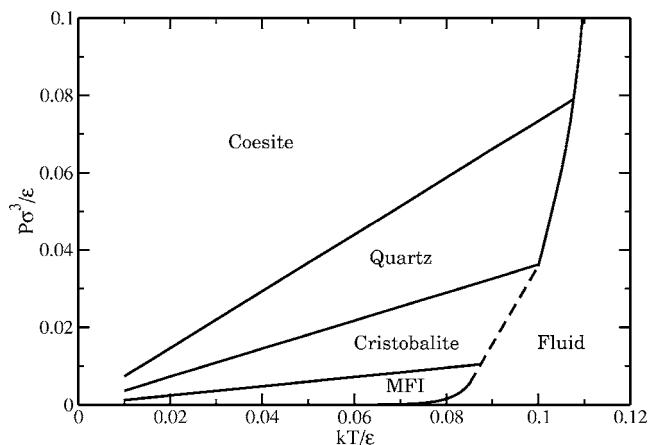


FIG. 2. Pressure ( $P\sigma^3/\epsilon$ ) vs temperature ( $k_B T/\epsilon$ ) phase diagram for our model of silica including the zeolite framework MFI. We find that MFI is stable at low pressure with respect to the dense phases of silica.

formed by having four template molecules inside a unit cell of the MFI framework. Because the separated template plays no role in the relative stabilities of pure silica phases, the boundaries between regions 1, 2, and 3 are determined by the pure silica phase diagram. Phase equilibrium between templated MFI and the separated template/silica phases ( $\alpha=1, 2, 3$ ), is determined from<sup>34</sup>

$$\mu_4[T_m(\text{SiO}_2)_n] = m\mu(T) + n\mu_\alpha(\text{SiO}_2), \quad (2.4)$$

where the left-hand-side of Eq. (2.4) is the chemical potential of templated MFI, while the right-hand-side contains the chemical potentials of pure template and pure silica phases. Pure template chemical potentials are obtained from the well-known equations of state of hard-sphere solids and fluids.<sup>32</sup> We draw an additional line passing through regions 2 and 3, marking the solid-fluid transition of the hard-sphere template. For the case of a template occupying the channel intersections in the MFI framework, the compound stoichiometry is  $T(\text{SiO}_2)_{24}$ .

### III. RESULTS AND DISCUSSION

#### A. Zeolite frameworks and the silica phase diagram: Isoenergetic model

We have calculated the silica phase diagram from our isoenergetic polymorph model, including silica zeolite frameworks MFI, SOD, LTA, and FAU. The framework densities of these materials are 18.4, 16.7, 14.2, and 13.3  $\text{SiO}_2$  units per 1000  $\text{\AA}^3$ , respectively. The resulting phase diagram is shown in Fig. 2.<sup>35</sup> The remarkable feature of this diagram is the appearance of MFI as a stable phase of our model at low pressures. As we mentioned earlier, this runs counter to the view that silica zeolite frameworks are metastable states. The other zeolite structures—SOD, LTA, and FAU—do not show any regime of thermodynamic stability based on our model calculations. Because all polymorphs have the same internal energy in this model, all phases are in equilibrium in the limit of zero temperature and pressure. Moreover, the relative stabilities are primarily determined by differences in

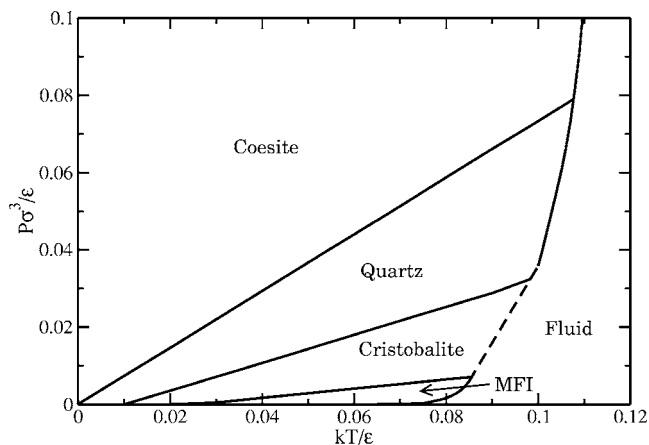


FIG. 3. Pressure ( $P\sigma^3/\epsilon$ ) vs temperature ( $k_B T/\epsilon$ ) phase diagram for our model of silica including the zeolite framework MFI. In this case differences in binding energies between the phases based on ground-state energies from DFT calculations are incorporated into the calculations.

$pV$ , making denser phases more stable at higher pressure. This may explain the instability of zeolite phases SOD, LTA, and FAU, which are less dense than MFI.

#### B. Zeolite frameworks and the silica phase diagram: Nondegenerate model

Now we consider how subtle differences in silica polymorph energies impact the phase diagram of our model. The phase diagram that arises from using Eq. (2.2) to compute polymorph energies is shown in Fig. 3. We see that MFI's region of stability in this recalculated phase diagram is pushed to elevated temperatures because of MFI's elevated lattice energy. Quartz and coesite are presumed to remain isoenergetic in this model because no DFT correction was calculated for coesite in Ref. 8. As such, the phase diagram in Fig. 3 predicts that these two phases remain in equilibrium in the limit of zero temperature and pressure.

The results of Johnson *et al.* on the thermodynamics of various silica polymorphs suggest that quartz is the stable polymorph of silica in air at standard temperature and pressure.<sup>3</sup> We note that the phase diagram in Fig. 3 correctly reproduces this fact. Johnson *et al.* measured Gibbs free energies of various silica phases at 298 and 1000 K; the results for silica MFI (relative to quartz) are 4.06 and 1.39 kJ/mol, respectively. These data suggest that MFI approaches thermodynamic stability at elevated temperatures. Indeed, assuming that the enthalpy and entropy of transformation from quartz to MFI are independent of temperature, the crossover temperature where MFI would become stable (relative to quartz) is 1360 K using the data of Johnson *et al.* Figure 3 shows that MFI is stable within our model above  $T^* = k_B T/\epsilon = 0.030$ , which corresponds to  $T = 1370$  K assuming that  $\epsilon = 380$  kJ per mol (Si-O bond dissociation energy). This remarkable agreement suggests that MFI may be the stable polymorph of silica above  $\sim 1400$  K. Experimental calorimetry in this elevated temperature range would be useful for testing our model prediction.

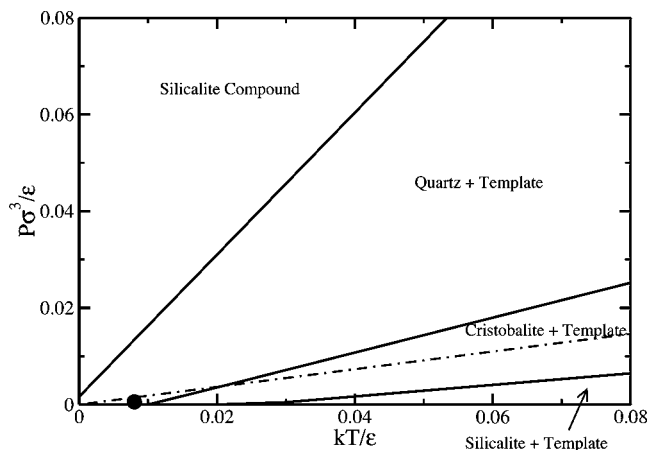


FIG. 4. Pressure-temperature phase diagram from our model for the system of silica+template molecules. The point represents approximately the experimental MFI synthesis conditions of 150 °C and 10 bar. The dot-dashed line in the cristobalite plus template region shows the transition from solid to fluid for the pure template (hard sphere) system (Ref. 36).

### C. Influence of hard sphere templating on the silica phase diagram

Figure 4 shows the pressure-temperature phase diagram arising from our hard-sphere model of the silica/template interaction. The key feature of this diagram is the appearance of templated MFI as a high-pressure stable phase. This result is consistent with the physics of our model, in which higher density phases become stable at high pressures. Templated MFI becomes the stable phase of this model at high pressure because, of the silica phases considered, only MFI can accommodate templates in its pores, hence responding to high pressure by increasing density. This result is not, however, consistent with a picture of the template stabilizing the MFI framework at synthesis temperatures. Indeed, within the assumptions of our hard-sphere templating model, we predict that the system of quartz+template remains the thermodynamically stable phase under typical experimental synthesis conditions ( $\sim 400$  K and 10 bar).

### D. Influence of hard sphere/attractive template on the silica phase diagram

Figure 5 shows the effect of a mean-field template-silica attraction on the model phase diagram of the silica+template system. From this diagram it can be seen that an attraction strength  $\epsilon_{TF}$  of nearly  $5\epsilon$  ( $\sim 1900$  kJ per mol template) is required to make the templated MFI phase thermodynamically stable at typical experimental synthesis conditions ( $\sim 400$  K and 10 bar). The strength of this template-framework attraction is *far higher* than experimentally measured template-framework enthalpies. Piccione *et al.* measured association enthalpies of several framework-template pairs.<sup>7</sup> For MFI, the most attractive template is tetrapropyl-ammonium (TPA), which exhibits an association enthalpy of  $-81 \pm 34$  kJ per mol TPA. This value suggests an attraction strength *much less* than 1900 kJ per mol. Our model calculations are thus inconsistent with a scenario where template-framework attractions establish the thermo-

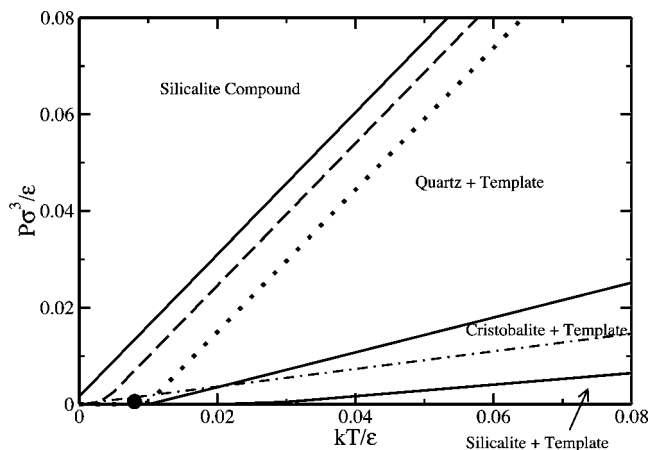


FIG. 5. Phase diagram of templated silica for various values of the template framework binding energy,  $\epsilon_{TF}$ : solid line,  $\epsilon_{TF}=0$ ; dashed line,  $\epsilon_{TF}=2\epsilon$ ; dotted line  $\epsilon_{TF}=5\epsilon$ . The point represents typical MFI synthesis conditions of 150 °C and 10 bar. The dot-dashed line in the cristobalite+template region shows the transition from solid to fluid for the pure template (hard sphere) system (Ref. 36).

dynamic stability of MFI under synthesis temperatures and pressures.

## IV. CONCLUDING REMARKS

We have applied our previously reported model of silica based on low coordination and strong association to the calculation of phase stability of silica zeolites SOD, LTA, MFI, and FAU. The efficiency of this model, which is based on hard-sphere repulsions and directed square-well attractions, allows free energy calculations for both dense and zeolitic polymorphs of silica. We applied the method of Frenkel and Ladd for calculating free energies of arbitrary solids. We found the surprising result that the all-silica MFI zeolite structure has a regime of thermodynamic stability in our model, relative to dense phases such as quartz. MFI is stable in our model at low pressures and above  $\sim 1400$  K. In contrast, our calculations predict that the less dense all-silica zeolites SOD, LTA, and FAU exhibit no regime of thermodynamic stability. This may begin to explain why silica MFI can be synthesized directly, while silica SOD, LTA, and FAU are typically prepared by post-synthesis de-alumination.

We have also used our model to investigate whether templating extends MFI's regime of thermodynamic stability to lower temperatures, by considering templates with hard-sphere repulsions and mean-field attractions to silica. Within the assumptions of our model, we find that quartz remains the thermodynamically stable polymorph at zeolite synthesis temperatures ( $\sim 400$  K) unless unphysically large template-silica attractions are assumed.

Our results suggest that some silica zeolites such as MFI may have regimes of thermodynamic stability, but not because of template stabilization. Experimental evidence shows that MFI is unstable with respect to quartz or cristobalite below 1000 K.<sup>3</sup> Our results suggest MFI becomes stable above 1400 K. New experimental information above 1000 K is needed to test our prediction regarding the thermodynamic stability of MFI.

Our model clearly lacks details such as solvent and charge, which may be crucial for a qualitative understanding of zeolite formation and stability. Nonetheless, our finding that some silica zeolites may be thermodynamically stable warrants further study with both experiments at higher temperatures and simulations with more realistic models.

## ACKNOWLEDGMENTS

The authors thank the referee for their very helpful suggestions. This work was supported by the National Science Foundation (CTS-0103010).

<sup>1</sup> *Handbook of Zeolite Science and Technology*, edited by S. M. Auerbach, K. A. Carrado, and P. K. Dutta (Dekker, New York, 2003).

<sup>2</sup> R. Singh and P. K. Dutta, in *Handbook of Zeolite Science and Technology*, edited by S. M. Auerbach, K. A. Carrado, and P. K. Dutta (Marcel Dekker, New York, 2003), pp. 21–64.

<sup>3</sup> G. K. Johnson, I. R. Tasker, D. A. Howell, and J. V. Smith, *J. Chem. Thermodyn.* **19**, 617 (1987).

<sup>4</sup> P. M. Piccione, C. Laberty, S. Yang, M. A. Camblor, A. Navrotsky, and M. E. Davis, *J. Phys. Chem. B* **104**, 10001 (2000).

<sup>5</sup> I. Petrovic, A. Navrotsky, M. E. Davis, and S. I. Zones, *Chem. Mater.* **5**, 1805 (1993).

<sup>6</sup> P. M. Piccione, B. F. Woodfield, J. Boerio-Goates, A. Navrotsky, and M. E. Davis, *J. Phys. Chem. B* **105**, 6025 (2001).

<sup>7</sup> P. M. Piccione, S. Yang, A. Navrotsky, and M. E. Davis, *J. Phys. Chem. B* **106**, 3629 (2002).

<sup>8</sup> R. Astala, S. M. Auerbach, and P. A. Monson, *J. Phys. Chem. B* **108**, 9208 (2004).

<sup>9</sup> K. de Boer, A. P. J. Jansen, and R. A. van Santen, *Phys. Rev. B* **52**, 12579 (1995).

<sup>10</sup> M. D. Foster, A. Simperler, R. G. Bell, O. D. Friedrichs, F. A. A. Paz, and J. Klinowski, *Nat. Mater.* **3**, 234 (2004).

<sup>11</sup> K. D. Hammonds, M. T. Dove, A. P. Giddy, V. Heine, and B. Winkler, *Am. Mineral.* **81**, 1057 (1996).

<sup>12</sup> N. J. Henson, A. K. Cheetham, and J. D. Gale, *Chem. Mater.* **6**, 1647 (1994).

<sup>13</sup> G. Sastre and A. Corma, *J. Phys. Chem. B* **110**, 17949 (2006).

<sup>14</sup> P. Vieillard, *Bull. Mineral.* **109**, 219 (1986).

<sup>15</sup> M. G. Wu and M. W. Deem, *J. Chem. Phys.* **116**, 2125 (2002).

<sup>16</sup> C. Baerlocher, W. M. Meier, and D. H. Olson, *Atlas of Zeolite Framework Types*, 5th ed. (Elsevier, Amsterdam, 2001); <http://www.iza-structure.org/databases>.

<sup>17</sup> M. H. Ford, S. M. Auerbach, and P. A. Monson, *J. Chem. Phys.* **121**, 8415 (2004).

<sup>18</sup> P. Vashishta, R. Kalia, and J. Rino, *Phys. Rev. B* **41**, 12197 (1990).

<sup>19</sup> J. Sauer and K. P. Schroder, *J. Phys. Chem.* **100**, 11325 (1996).

<sup>20</sup> S. Tsuneyuki, M. Tsukada, H. Aoki, and Y. Matsui, *Phys. Rev. Lett.* **61**, 869 (1988).

<sup>21</sup> B. W. H. van Beest, G. J. Kramer, and R. A. van Santen, *Phys. Rev. Lett.* **64**, 1955 (1990).

<sup>22</sup> B. Vessal, M. Leslie, and C. R. A. Catlow, *Mol. Simul.* **3**, 123 (1989).

<sup>23</sup> D. Ghonasgi and W. G. Chapman, *Mol. Phys.* **79**, 291 (1993).

<sup>24</sup> J. Kolafa and I. Nezbeda, *Mol. Phys.* **61**, 161 (1987).

<sup>25</sup> D. Frenkel and A. J. C. Ladd, *J. Chem. Phys.* **81**, 3188 (1984).

<sup>26</sup> O. A. Fouad, R. M. Mohamed, M. S. Hassan, and I. A. Ibrahim, *Catal. Today* **116**, 82 (2006).

<sup>27</sup> S. I. Zones, S. J. Hwang, S. Elomari, I. Ogino, M. E. Davis, and A. W. Burton, *C. R. Chim.* **8**, 267 (2005).

<sup>28</sup> A. Burton, R. J. Darton, M. E. Davis, S. J. Hwang, R. E. Morris, I. Ogino, and S. I. Zones, *J. Phys. Chem. B* **110**, 5273 (2006).

<sup>29</sup> D. J. Willock, D. W. Lewis, C. R. A. Catlow, G. J. Hutchings, and J. M. Thomas, *J. Mol. Catal. Chem.* **119**, 415 (1997).

<sup>30</sup> S. Caratzoulas, D. G. Vlachos, and M. Tsapatsis, *J. Am. Chem. Soc.* **128**, 596 (2006).

<sup>31</sup> T. Moeller, *Inorganic Chemistry: A Modern Introduction* (Wiley Interscience, New York, 1982).

<sup>32</sup> P. A. Monson and D. A. Kofke, *Adv. Chem. Phys.* **115**, 113 (2000).

<sup>33</sup> M. D. Eldridge, P. A. Madded, and D. Frenkel, *Mol. Phys.* **80**, 987 (1993).

<sup>34</sup> X. Cottin and P. A. Monson, *J. Chem. Phys.* **102**, 3354 (1995).

<sup>35</sup> There was a numerical error in the calculation of the quartz-cristobalite equilibrium in our earlier work. This led to a lower slope for the quartz-cristobalite equilibrium line than shown here. However, the qualitative prediction is unchanged.

<sup>36</sup> W. G. Hoover and F. H. Ree, *J. Chem. Phys.* **49**, 3609 (1968).